

Robust estimation of deformation from observation differences for free control networks

Krzysztof Nowel · Waldemar Kamiński

Received: 22 May 2013 / Accepted: 8 April 2014 / Published online: 9 May 2014
© The Author(s) 2014. This article is published with open access at Springerlink.com

Abstract Deformation measurements have a repeatable nature. This means that deformation measurements are performed often with the same equipment, methods, geometric conditions and in a similar environment in epochs 1 and 2 (e.g., a fully automated, continuous control measurements). It is, therefore, reasonable to assume that the results of deformation measurements can be distorted by both random errors and by some non-random errors, which are constant in both epochs. In other words, there is a high probability that the difference in the accuracy and precision of measurement of the same geometric element of the network in both epochs has a constant value and sign. The constant errors are understood, but the manifestation of these errors is difficult to determine in practice. For free control networks (the group of potential reference points in absolute control networks or the group of potential stable points in relative networks), the results of deformation measurements are most often processed using robust methods. Classical robust methods do not completely eliminate the effect of constant errors. This paper proposes a new robust alternative method called REDOD. The performed tests showed that if the results of deformation measurements were additionally distorted by constant errors, the REDOD method completely eliminated their effect from deformation analysis results. If the results of deformation measurements are only distorted by random errors, the REDOD method yields very similar deformation analysis results as the classical IWST method. The numerical tests were preceded by a theoretical part. The theoretical part

describes the algorithm of classical robust methods. Particular attention was paid to the IWST method. In relation to classical robust methods, the optimization problem of the new REDOD method was formulated and the algorithm for its solution was derived.

Keywords Robust estimation · Stability of reference points · Displacement · S-transformation · IWST · REDOD

1 Introduction

Absolute and relative control networks are distinguished in deformation measurements and analysis. Absolute control networks consist of controlled points placed on the surveyed object (e.g., on a dam, bridge) and potential reference points usually placed outside the effect of factors causing deformations. Relative control networks consist only of controlled points established on the surveyed object (e.g., on an area covered by mining damage). Both potential reference points of absolute networks and potential stable points of relative networks (the points are on a potentially rigid network fragment) form FCN (free control networks). The problem of deformation analysis for FCN is, in fact, the problem of identifying the mutual stability of these network points. In this way, the datum for the displacement vector of all absolute or relative control network points is defined. It can be seen that deformation analysis for FCN is, therefore, an essential task in deformation analysis for control networks (Chen 1983; Caspary 2000; Denli 2008).

Methods of deformation analysis for FCN described in literature can be classified according to different criteria. In this paper, they are divided into robust methods and non-robust methods (Chrzanowski and Chen 1990; Caspary 2000; Setan and Singh 2001). Today, the robust methods are applied more

K. Nowel (✉) · W. Kamiński
Institute of Geodesy, University of Warmia and Mazury in Olsztyn,
1 Oczapowskiego Str., 10-719 Olsztyn, Poland
e-mail: krzysztof.nowel@uwm.edu.pl

W. Kamiński
e-mail: waldemar.kaminski@uwm.edu.pl

often. It should be stressed that “robust” does not refer here to outliers in observations; “robust” refers here to single-point movements. The observations must be clean of outliers. This is very important. Classical robust methods are based on the results of separate adjustments by the least squares (LS) method of two measurement epochs, i.e., on adjusted coordinates. These methods consist in S-transformation (Helmert similarity transformation) of differences in these coordinates with the optimization condition of robust estimation. The obtained displacement vectors of single points are assessed statistically for significance. The best-known methods from this group include the iterative weighted similarity transformation (IWST) method, which fulfills the condition of the minimum sum of absolute component values of displacement vectors (Chen 1983; Chen et al. 1990; Setan and Singh 2001; Setan and Othman 2006; Gökalp and Taşçi 2009) and the least absolute sum (LAS) method, which fulfills the condition of the minimum sum of length values of displacement vectors (Caspary 1984; Caspary and Borutta 1987; Caspary et al. 1990; Setan and Singh 2001). Proposals for the use of other optimization conditions, e.g., the minimum objective function of the Huber method or the Danish method, can also be found in literature (Caspary and Borutta 1987). The IWST method serves as the prototype for classical robust methods. The other robust methods are only modifications, differing in the optimization condition used. The non-robust methods are also based on the results of separate adjustments by the LS method of two measurement epochs, i.e., on adjusted coordinates. Statistical tests are most popular in this group, e.g., the congruency test (Niemeier 1981; Setan and Singh 2001; Denli and Deniz 2003). The congruency test method consists in finding the most numerous possible group of points for which the value of the displacement test statistic does not exceed the critical value. Displacement vectors are computed on the basis of S-transformation of differences in adjusted coordinates of these points with the optimization condition of the LS method or on the basis of differences in coordinates obtained from free adjustments by the LS method. Although many more other new methods for deformation analysis, e.g., robust method based on M_{split} estimation (Wiśniewski 2009; Duchnowski and Wiśniewski 2012) or R estimation (Duchnowski 2010, 2013) or the non-robust Fredericton approach (Gökalp and Taşçi 2009), can be found in literature, this paper is limited to the presentation of only the most common solutions.

Geodetic methods are most often used to measure minor deformations with values slightly exceeding errors in their measurement. A special role in deformation analysis is, therefore, played by the quality of results, i.e., the accuracy of the determined displacement vectors and the correct assessment of their statistical significance (effectiveness). The quality of deformation analysis results is conditioned by the measurement precision (random errors) and the measurement reli-

bility and the processing of the results. A higher reliability level of a measurement produces a lower risk of making gross and systematic errors. A high measurement reliability level is achieved by, among others, periodical instrument checks, the use of self-checking measurement procedures and the introduction of corrections due to the disturbing effects of external conditions. The higher the reliability level of the processing of measurement results, the higher the probability will be of detecting possible gross and systematic errors (internal reliability) and the lower the effect of these undetected errors will be on the quality of deformation analysis results (external reliability), e.g., Caspary (2000), Prószyński (2010).

Deformation measurements are performed at different moments of time, but often with the same equipment, methods, geometric conditions and in a similar environment in epochs 1 and 2. Moreover, the same instrument and target are most often set on given points in both epochs. It is, therefore, reasonable to assume that the results of deformation measurements can be distorted both by random errors and by some non-random errors, which are constant in both epochs, i.e., errors with the same value and the same sign in both epochs. This means that the error of measurement of the same geometric element of the network in both epochs may contain a common factor, which is constant in both epochs. This factor is, in fact, the difference in the measurement accuracy and precision. The constant errors are understood, but the manifestation of these errors is difficult to determine in practice. Classical deformation analysis of FCN is most often performed by robust methods. In these methods, the displacement vector is determined in robust S-transformation of differences in adjusted coordinates. This approach does not completely eliminate the effect of constant errors and, therefore, leads to reduced external reliability level of processing and, consequently, to reduced quality of deformation analysis results. Moreover, the displacement vector and its covariance matrix are estimated separately in two different computational processes. As a result, the displacement vector estimator and its covariance matrix estimator have different stochastic properties, i.e., the actual and estimated accuracy of the displacement vector estimator is different.

In the 1970s, the Polish geodesist Prof. Tadeusz Lazzarini dealt with this problem for control networks with a defined datum. Prof. Lazzarini developed a method for joint estimation of the displacement vector and its covariance matrix directly from differences in unadjusted observations (Lazzarini et al. 1977; Chrzanowski and Chen 1990). This approach completely solves, among others, the problem of the effect of constant errors and the problem of discrepancy between the actual and estimated accuracy of the displacement vector estimator. This method is still used successfully in deformation analysis of control networks with a defined datum, among others in an automated system for continuous control measurements ALERT (Wilkins et al. 2003). Mod-

ern robust estimation and matrix g-inverse theory allow this approach to be expanded to FCN (control networks without a defined datum). Such expansion is the aim of this paper. In fact, a new robust method for FCN deformation analysis will be developed and examined in this paper, in which the displacement vector will be determined in the process of robust M estimation of differences in unadjusted observations. The proposed method was conventionally called robust estimation of deformation from observation differences (REDOD).

2 Robust transformation of deformation from coordinate differences

The robust FCN deformation analysis method proposed in this paper will be developed based on classical robust methods and is specifically based on the IWST method. Therefore, the algorithm of classical robust methods was derived and described in this section. Particular attention was paid to the IWST method.

As previously mentioned, in classical methods the displacement vector is determined in the process of robust S-transformation of the differences in adjusted coordinates. Generally, the algorithm always consists of the following three steps.

2.1 Step 1: LS estimation of the vector of coordinates

LS estimation of the vector of coordinates is carried out separately for each measurement epoch. The computations cannot distort measurement results or the relationships occurring between them. The basic aim is to provide data for starting robust transformation. The result of this processing is the vector of adjusted coordinates for all analyzed points in an FCN

$$\hat{\mathbf{x}} = \mathbf{x}^0 + \hat{\delta}_{\mathbf{x}}, \tag{1}$$

where $\mathbf{x}^0 \in \mathfrak{R}^{u \times 1}$ is the vector of the approximate coordinates (the same in both epochs) and $\hat{\delta}_{\mathbf{x}} \in \mathfrak{R}^{u \times 1}$ is the LS estimator of the vector of the corrections to the approximate coordinates.

The functional model, which is the linearized form of the initial nonlinear relationships, has the form

$$\mathbf{l}^{\text{obs}} - \mathbf{l}^0 + \mathbf{v} = \mathbf{A}\delta_{\mathbf{x}}, \quad \mathbf{l}^{\text{obs}} \sim N(\mathbf{A}\mathbf{x}, \mathbf{C}), \tag{2}$$

where $\mathbf{A} \in \mathfrak{R}^{n \times u}$ is the design matrix, $\mathbf{l}^0 \in \mathfrak{R}^{n \times 1}$ is the vector of approximate observations, $\mathbf{l}^{\text{obs}} \in \mathfrak{R}^{n \times 1}$ is the vector of actual observations, $\mathbf{v} \in \mathfrak{R}^{n \times 1}$ is the vector of residuals of observations and $\mathbf{C} \in \mathfrak{R}^{n \times n}$ is the covariance matrix of observations. The sought parameter vector estimator has the form

$$\hat{\delta}_{\mathbf{x}} = \mathbf{Q}_{\hat{\mathbf{x}}}\boldsymbol{\omega}, \tag{3}$$

where $\boldsymbol{\omega} = \mathbf{A}^T\mathbf{P}(\mathbf{l}^{\text{obs}} - \mathbf{l}^0)$, $\mathbf{P} \in \mathfrak{R}^{n \times n}$ is the weight matrix of observations, $\mathbf{Q}_{\hat{\mathbf{x}}} = \mathbf{N}^-$ is the cofactor matrix of the vector of

adjusted coordinates and $\mathbf{N}^- = (\mathbf{A}^T\mathbf{P}\mathbf{A})^-$ is any g-inverse, fulfilling the property $\mathbf{N}\mathbf{N}^-\mathbf{N} = \mathbf{N}$. The network is a free network. In this case, the network has a datum defect

$$de = u - \text{rank}(\mathbf{A}), \quad \text{rank}(\mathbf{A}) = r < u \tag{4}$$

the matrix \mathbf{A} is the matrix of the columnarily incomplete rank and, therefore, the ordinary (classical) inverse \mathbf{N}^{-1} will not be determined. The g-inverse determination methods are well-described in literature (e.g., Rao 1973; Caspary 2000). For example, one of the g-inverses can be determined in a simple, algebraic manner, by representation of the design matrix in the following form

$$\mathbf{A} = [\mathbf{A}_1 \quad \mathbf{A}_2], \tag{5}$$

where $\mathbf{A}_1 \in \mathfrak{R}^{n \times r}$, $r = \text{rank}(\mathbf{A}_1) = \text{rank}(\mathbf{A})$ and $\mathbf{A}_2 \in \mathfrak{R}^{n \times de}$ is, in fact, the matrix defining the datum for the geodetic network. The final result of step 1 is the vectors $\hat{\mathbf{x}}_{(e)}$ (1) and their cofactor matrices $\mathbf{Q}_{\hat{\mathbf{x}}_{(e)}}$, where e is the number of the measurement epoch.

Of course, during LS estimation of the vector of coordinates, other important aspects that need to be considered are outlier detection (observations) (e.g., Baarda's data snooping, Pope's test or some robust estimation) and tests of the compatibility between the two epochs (variance ratio test). Moreover, in the case of heterogeneous networks, it is sometimes important to perform the estimation of the variance and covariance components.

2.2 Step 2: robust S-transformation of the displacement vector

Displacements of individual points in an FCN cannot be determined on the basis of differences in the direct values of the vectors $\hat{\mathbf{x}}_{(1)}$ and $\hat{\mathbf{x}}_{(2)}$. LS estimation of the vector of coordinates can concern networks with different datum defect types in both epochs (because of different types of observations). Moreover, constraints defining the datum for the geodetic network in epochs 1 and 2 can concern different points (e.g., because of damage to some points in epoch 2) or can concern the same unstable points. For this reason, the datum for the geodetic network in epoch 2 can be freely shifted, rotated and re-scaled in relation to the datum in epoch 1 (Chen 1983; Chen et al. 1990). The vector $\hat{\mathbf{x}}_{(2)}$ can, therefore, be adjusted in a different datum than the vector $\hat{\mathbf{x}}_{(1)}$ and this is why

$$\mathbf{d} \neq \hat{\mathbf{x}}_{(2)} - \hat{\mathbf{x}}_{(1)}, \tag{6}$$

where $\mathbf{d} \in \mathfrak{R}^{u \times 1}$ is the vector of displacement components for all analyzed points in an FCN. This difference $\hat{\mathbf{x}}_{(2)} - \hat{\mathbf{x}}_{(1)}$ is the so-called apparent (or raw) displacement vector.

To reduce the vectors $\hat{\mathbf{x}}_{(1)}$ and $\hat{\mathbf{x}}_{(2)}$ to a common datum, the vector $\hat{\mathbf{x}}_{(2)}$ is transformed to the datum of the vector $\hat{\mathbf{x}}_{(1)}$. This task consists in fitting the vector $\hat{\mathbf{x}}_{(2)}$ into the vector

$\hat{\mathbf{x}}_{(1)}$ reduced to the center of gravity of the network. The transformed vector $\hat{\mathbf{x}}'_{(2)}$ has the form

$$\hat{\mathbf{x}}'_{(2)} = \hat{\mathbf{x}}_{(2)} - \mathbf{H}\mathbf{t} \quad (7)$$

because $\hat{\mathbf{x}}_{(2)} = \hat{\mathbf{x}}'_{(2)} + \mathbf{H}\mathbf{t}$, where $\mathbf{t} \in \mathfrak{R}^{h \times 1}$ is the vector of S-transformation parameters, i.e., translation, rotation, scale distortion, h designates the number of all datum parameters of a given network and \mathbf{H} is the design matrix of S-transformation to a common datum (epoch 1). For example, for a 2-D network, the matrix \mathbf{H} has the form

$$\mathbf{H} \in \mathfrak{R}^{2m \times h} = \begin{bmatrix} \vdots & \vdots & \vdots & \vdots \\ 1 & 0 & -\bar{y}_{i(1)} & \bar{x}_{i(1)} \\ 0 & 1 & \bar{x}_{i(1)} & \bar{y}_{i(1)} \\ \vdots & \vdots & \vdots & \vdots \end{bmatrix}, \quad (8)$$

where m designates the number of points in a given network and $\bar{x}_{i(1)}$, $\bar{y}_{i(1)}$ designate adjusted coordinates of point i in epoch 1 reduced to the center of gravity of the network. The first two columns refer to translation along the axes X , Y , respectively, the third column refers to rotation around the axis Z and the last column refers to scale distortion. More theory on that issue (among others, the matrix \mathbf{H} for a 1-D and 3-D network) can be found in papers by [Chen \(1983\)](#), [Caspary \(2000\)](#) and [Even-Tzur \(2011\)](#).

Since the displacement vector now has the form $\mathbf{d} = \hat{\mathbf{x}}'_{(2)} - \hat{\mathbf{x}}_{(1)}$, consequently $\mathbf{d} = (\hat{\mathbf{x}}_{(2)} - \hat{\mathbf{x}}_{(1)}) - \mathbf{H}\mathbf{t}$. Of course, this system of equations has infinitely many solutions for the displacement vector. To obtain a unique, sought value of this vector, we also need to formulate proper objective functions.

Let us recall that FCN may consist of potential reference points of absolute networks or potential stable points of relative networks. Hence, we can assume that most of these points (more than half) are actually stable. Unfortunately, there is a risk that single unstable points may occur among this group. It can be assumed that measurement errors at all epochs are a sample of random variables with a normal distribution with a mean of zero and accepted standard deviation. In this case, the estimated displacements of actually stable points should also be a sample of random variables with such a distribution and the estimated displacements of actually unstable points should be random variables which are the outliers of this distribution. In other words, the vector of displacement components of FCN points may have a contaminated normal distribution (analogously as, e.g., a vector of observations with suspected gross errors). This is why the robust objective functions are very useful in deformation analysis for FCN. Thus, "outliers" do not refer here to the observations. "Outliers" refer here to the single-point movements. It should be stressed that if all of the FCN points are certainly actually stable, then the LS and robust methods lead to unbiased results, but robust methods are less efficient

and yield greater variances. This decrease in efficiency is the price to be paid for the robustness of the method.

In the IWST method, the objective function is the L_1 -norm of vector \mathbf{d} , i.e., ([Chen 1983](#); [Chen et al. 1990](#); [Setan and Singh 2001](#); [Setan and Othman 2006](#); [Gökalp and Tasçi 2009](#)). The optimization problem of the IWST method has the following form

$$\left. \begin{array}{l} \mathbf{d} = (\hat{\mathbf{x}}_{(2)} - \hat{\mathbf{x}}_{(1)}) - \mathbf{H}\mathbf{t} \quad \text{functional model} \\ \psi(\mathbf{t}) = \|\mathbf{d}\|_1 = \sum |d_i| = \min \quad \text{optimization condition} \end{array} \right\},$$

↓
definition of the datum for the displacement vector

(9)

where $\mathbf{d} = [d_1, \dots, d_u]^T$, d_i is the given component of vector \mathbf{d} for point i (dx_i or dy_i or dz_i), u is the number of the displacement components for all m analyzed points in an FCN. The final solution to the optimization problem of the IWST method has the following iterative form

$$\left. \begin{array}{l} \hat{\mathbf{d}}^{(k)} = \mathbf{S}^{(k)} (\hat{\mathbf{x}}_{(2)} - \hat{\mathbf{x}}_{(1)}) \\ \mathbf{Q}_{\hat{\mathbf{d}}}^{(k)} = \mathbf{S}^{(k)} (\mathbf{Q}_{\hat{\mathbf{x}}_{(1)}} + \mathbf{Q}_{\hat{\mathbf{x}}_{(2)}}) (\mathbf{S}^{(k)})^T \\ \mathbf{W}^{(k+1)} = \text{diag}(\dots, w_i^{(k+1)}, \dots) \end{array} \right\}_{k=1,2,\dots} \quad (10)$$

where $\mathbf{S}^{(k)} = \mathbf{I} - \mathbf{H}(\mathbf{H}^T \mathbf{W}^{(k)} \mathbf{H})^{-1} \mathbf{H}^T \mathbf{W}^{(k)}$ is the matrix of S-transformation of the displacement vector to a common datum in epoch 1, $\mathbf{W}^{(k=1)} = \mathbf{I}$, $\mathbf{I} \in \mathfrak{R}^{u \times u}$ is the identity matrix and

$$w_i^{(k+1)} = 1 / \left| \hat{d}_i^{(k)} \right| \quad (11)$$

It is possible that during the iterations (10) some $\hat{d}_i^{(k)}$ may approach zero, causing numerical instabilities, because $1 / \left| \hat{d}_i^{(k)} \right|$ becomes very large. For this reason in practice, Eq. (11) is replaced with the equation

$$w_i^{(k+1)} = 1 / \left(\left| \hat{d}_i^{(k)} \right| + c \right), \quad (12)$$

where c is the precision for computations, e.g., 0.0001 m. Proposals for uses of other solutions in this task can be found in other papers, e.g., [Marx \(2013\)](#). The iterative process (10) is finished when all components of the difference $\left| \hat{\mathbf{d}}^{(k+1)} - \hat{\mathbf{d}}^{(k)} \right|$ are lower than the adopted precision for computations c (convergence). The final robust estimator of the vector of displacement components for all analyzed points in an FCN, i.e., vector $\hat{\mathbf{d}}^R$ and the final cofactor matrix of this vector, i.e., the matrix $\mathbf{Q}_{\hat{\mathbf{d}}^R}$, is obtained from the last iterative step. Vector $\hat{\mathbf{d}}^R$ consists of vectors $\hat{\mathbf{d}}_i^R$ for single points in an FCN, i.e., $(\hat{\mathbf{d}}^R)^T = [\dots, (\hat{\mathbf{d}}_i^R)^T, \dots]$, and the matrix $\mathbf{Q}_{\hat{\mathbf{d}}^R}$, neglecting the correlation between the points and contains cofactor matrices of these vectors, i.e., $\mathbf{Q}_{\hat{\mathbf{d}}^R} = \text{diag}(\dots, \mathbf{Q}_{\hat{\mathbf{d}}_i^R}, \dots)$. Proposals for uses of other objective

functions $\psi(\mathbf{t})$ in this task (among others, the objective function of the LAS method, the Huber method or the Danish method) can be found in papers by Caspary and Borutta (1987), Caspary et al. (1990), Setan and Singh (2001).

2.3 Step 3: assessment of the significance of the displacement vector

All $\hat{\mathbf{d}}_i^R$ vectors are assessed statistically for significance. The aim of this assessment is to check if these vectors are actually displacements or only the result of random measurement errors. The first step consists in checking the global significance test

$$T = \frac{(\hat{\mathbf{d}}^R)^T \mathbf{Q}_{\hat{\mathbf{d}}^R}^+ (\hat{\mathbf{d}}^R)}{u \hat{\sigma}_0^2} < F(\alpha, u, f), \tag{13}$$

where

$$\hat{\sigma}_0^2 = \left(\hat{\mathbf{v}}_{(1)}^T \mathbf{P}_{(1)} \hat{\mathbf{v}}_{(1)} + \hat{\mathbf{v}}_{(2)}^T \mathbf{P}_{(2)} \hat{\mathbf{v}}_{(2)} \right) / f \tag{14}$$

is the pooled variance factor estimator for both epochs and $\hat{\mathbf{v}}_{(e)} = \mathbf{A} \hat{\mathbf{d}}_{\mathbf{x}_{(e)}} - (\mathbf{I}_{(e)}^{\text{obs}} - \mathbf{I}^0)$, $f = f_{(1)} + f_{(2)}$, $f_{(e)} = n_{(e)} - u_{(e)} + de_{(e)}$, α is the significance level, i.e., the probability of making a Type I error in testing statistical, $u = \text{rank}(\mathbf{Q}_{\hat{\mathbf{d}}^R})$ and F is the critical value read from Fisher’s cumulative distribution function (Aydin 2013). If the global test passes, this means that all $\hat{\mathbf{d}}_i^R$ vectors are not statistically significant and, thus, these points can be regarded as actually stable. In the opposite case, localization of single-point displacements is then performed. The single-point test, neglecting the correlation between the points, is

$$T_i = \frac{(\hat{\mathbf{d}}_i^R)^T \mathbf{Q}_{\hat{\mathbf{d}}_i^R}^{-1} (\hat{\mathbf{d}}_i^R)}{u_i \hat{\sigma}_0^2} < F(\alpha, u_i, f), \tag{15}$$

where $u_i = \text{rank}(\mathbf{Q}_{\hat{\mathbf{d}}_i^R})$ is the number of the dimension of the single-point displacement vector (1 or 2 or 3) (Chen 1983; Setan and Singh 2001). Instead of the local test (15), neglecting the correlation between the points, one can also apply the local test based on the decorrelated matrix $\mathbf{Q}_{\hat{\mathbf{d}}_i^R}$. More details are given in Caspary (2000). If the single-point test passes, this means that the displacement of point i is not statistically significant and, thus, this point can be regarded as actually stable. In the opposite case, this point can be regarded as unstable. The solution (15) can be used for 1-D, 2-D and 3-D networks. Moreover, another condition can be derived from the condition (15) for better interpretation of results

$$\hat{\mathbf{d}}_i^R \in E = f \left(F, \hat{\sigma}_0^2, \mathbf{Q}_{\hat{\mathbf{d}}_i^R} \right), \tag{16}$$

where E is the confidence interval (1-D network) or the set of points formed by the confidence ellipse (2-D network), (e.g., Kamiński and Nowel 2013) or the confidence ellipsoid (3-D

network) (e.g., Cederholm 2003). In this case, the significance assessment consists in checking graphically whether the vector $\hat{\mathbf{d}}_i^R$ does not exceed the confidence interval for determination of this vector (1-D network) or the confidence ellipse for determination of this vector (2-D network) or the confidence ellipsoid for determination of this vector (3-D network). Of course, both solutions (15), (16) give the same results.

It should be stressed that the matrix $\mathbf{Q}_{\hat{\mathbf{d}}^R}$ is approximate since the relation between $\hat{\mathbf{x}}_{(2)} - \hat{\mathbf{x}}_{(1)}$ and $\hat{\mathbf{d}}^R$ is nonlinear according to (10). Thus, the law of variance propagation does not apply. In this case, the proper cofactor matrix can, of course, be determined only by the Monte Carlo approach (e.g., Du Mond and Lenth 1987). Moreover, the assumption that the T_i statistic has Fisher’s distribution is also approximate based on the assumption $\hat{\mathbf{d}}^R \sim N$. The relation between $(\hat{\mathbf{x}}_{(2)} - \hat{\mathbf{x}}_{(1)}) \sim N$ and $\hat{\mathbf{d}}^R$ is nonlinear and, therefore, the estimator $\hat{\mathbf{d}}^R$ does not have a normal distribution. The distribution of this estimator is not known and the initial assumption $\hat{\mathbf{d}}^R \sim N$ is only approximate. Consequently, the assumptions $(\hat{\mathbf{d}}_i^R)^T \mathbf{Q}_{\hat{\mathbf{d}}_i^R}^{-1} (\hat{\mathbf{d}}_i^R) \sim \chi^2$ and $T_i \sim F$ are also approximate, although the approximate F tests (13, 15, 16) are accepted.

3 Robust estimation of deformation from observation differences

As previously mentioned, classical robust methods for deformation analysis of FCN are based on the results of separate adjustments of observations for epochs 1 and 2, i.e.,

$$\begin{array}{l} \mathbf{I}_{(1)}^{\text{obs}} \xrightarrow{\text{LS estimation}} \hat{\mathbf{x}}_{(1)} \\ \hspace{15em} \xrightarrow{\text{robust S-transformation}} \hat{\mathbf{d}}^R \\ \mathbf{I}_{(2)}^{\text{obs}} \xrightarrow{\text{LS estimation}} \hat{\mathbf{x}}_{(2)} \end{array}$$

The basis for such an approach is the assumption that vector \mathbf{d} is the difference in functions of independent observations ($\mathbf{d} = f(\mathbf{I}_{(2)}^{\text{obs}}) - f(\mathbf{I}_{(1)}^{\text{obs}})$). If the observations are distorted in both epochs only by random errors, then such an approach is correct, but not if observations are additionally distorted by constant errors.

First (and most importantly), separate adjustments fulfill the condition for the closing of geometric figures, which is not significant in the deformation analysis process. Such a procedure, in the case of the occurrence of constant errors, leads to an unjustified increase in the values of the vectors $\hat{\mathbf{v}}_{(1)}$, $\hat{\mathbf{v}}_{(2)}$ and, thus, the factor $\hat{\sigma}_0^2$ (14) and, consequently, may lead to incorrect assessment of the statistical significance of the $\hat{\mathbf{d}}_i^R$ vectors (13), (15) or (16). Second, if the matrices $\mathbf{P}_{(1)}$, $\mathbf{P}_{(2)}$ are not proportional in both epochs (e.g., for GNSS vectors), vector $\hat{\mathbf{d}}^R$ will be distorted by the effect of constant errors. These errors will not cancel out completely in the iterative process (10) because, in this case, their effect on the values

of the vectors $\hat{\mathbf{x}}_{(1)}$, $\hat{\mathbf{x}}_{(2)}$ (1) will be different. As a result, the vector $\hat{\mathbf{d}}^R$ will be partly distorted by their effect. Third, the vector $\hat{\mathbf{d}}^R$ and the factor $\hat{\sigma}_0^2$ are estimated independently, in two different computational processes. As a result, the vector $\hat{\mathbf{d}}^R$ and the factor $\hat{\sigma}_0^2$ have different stochastic properties. This discrepancy may lead to incorrect assessment of the statistical significance of the vectors $\hat{\mathbf{d}}_i^R$.

As mentioned in the introduction, when the displacement vector is determined directly from differences in unadjusted observations, the above problems do not occur. Therefore, this paper proposes a new robust alternative method for deformation analysis of FCN (REDOD). The basis of this method is the assumption that vector \mathbf{d} is a function of differences in independent observations ($\mathbf{d} = f(\mathbf{I}_{(2)}^{\text{obs}} - \mathbf{I}_{(1)}^{\text{obs}})$), i.e.,

$$(\mathbf{I}_{(2)}^{\text{obs}} - \mathbf{I}_{(1)}^{\text{obs}}) \xrightarrow{\text{robust estimation}} \hat{\mathbf{d}}^R$$

If observations in both epochs are additionally distorted by constant errors, such an approach can eliminate the effect of these errors from deformation analysis results. As a result of estimation, the vector of differences in observations is assigned only such a vector of residuals which enables determination of vector $\hat{\mathbf{d}}^R$, but “does not bend” observations to fulfill the conditions for the closing of geometric figures. An unjustified increase in the value of the factor $\hat{\sigma}_0^2$ (14) and distortions of vector $\hat{\mathbf{d}}^R$ are avoided this way. Moreover, the vector $\hat{\mathbf{d}}^R$ and the factor $\hat{\sigma}_0^2$ are estimated in the same computational process and, as a consequence, have the same stochastic properties.

The algorithm of the proposed REDOD method consists of the following two steps.

3.1 Step 1: robust estimation of the displacement vector

It can be seen that if the same geometric network elements have been measured at both analyzed epochs, then $\mathbf{A}_{(1)} = \mathbf{A}_{(2)} = \mathbf{A}$, e.g., for continuous control measurements. In this case, it is possible to construct a certain alternative and very natural deformation model, in which the vector of observation differences will be the vector of “observations” and the sought displacement vector will be the vector of parameters. If interepoch observations, which are described by the model (2), are subtracted from each other, we will obtain for two epochs $(\mathbf{I}_{(2)}^{\text{obs}} - \mathbf{I}^0) + \mathbf{v}_{(2)} - (\mathbf{I}_{(1)}^{\text{obs}} - \mathbf{I}^0) - \mathbf{v}_{(1)} = \mathbf{A}\delta_{\mathbf{x}_{(2)}} - \mathbf{A}\delta_{\mathbf{x}_{(1)}}$ and then

$$(\mathbf{I}_{(2)}^{\text{obs}} - \mathbf{I}_{(1)}^{\text{obs}}) + \mathbf{v}_{\Delta} = \mathbf{A}\mathbf{d}, \quad (\mathbf{I}_{(2)}^{\text{obs}} - \mathbf{I}_{(1)}^{\text{obs}}) \sim N(\mathbf{A}\mathbf{d}, \mathbf{C}_{\Delta}) \quad (17)$$

because $\delta_{\mathbf{x}_{(2)}} - \delta_{\mathbf{x}_{(1)}} = \mathbf{d}$, $\mathbf{v}_{\Delta} = \mathbf{v}_{(2)} - \mathbf{v}_{(1)}$, $\mathbf{C}_{\Delta} \in \mathfrak{R}^{n \times n}$ is the covariance matrix of differences in observations (Lazarini et al. 1977). Because the vector of displacement components of FCN points may have a contaminated normal distribution with a mean of zero and accepted standard deviation,

the solution to the system of Eq. (17) should be a robust estimator of vector \mathbf{d} . In the REDOD method, as in the IWST method, the L_1 -norm estimator of vector \mathbf{d} will be used for this purpose. Moreover, because errors of geodetic observations are of random nature (according to normal distribution), the robust estimator of vector \mathbf{d} should simultaneously fulfill the optimization condition of the LS method for the vector of residuals of differences in observations. Consequently, the following optimization problem for the system of Eq. (17) is obtained

$$\left. \begin{aligned} \mathbf{v}_{\Delta} &= \mathbf{A}\mathbf{d} - (\mathbf{I}_{(2)}^{\text{obs}} - \mathbf{I}_{(1)}^{\text{obs}}) && \text{functional model} \\ \mathbf{C}_{\Delta} &= \sigma_0^2 \mathbf{Q}_{\Delta} = \sigma_0^2 \mathbf{P}_{\Delta}^{-1} && \text{stochastic model} \\ \phi(\mathbf{d}) &= \mathbf{v}_{\Delta}^T \mathbf{P}_{\Delta} \mathbf{v}_{\Delta} = \min && \text{optimization condition} \\ \psi(\mathbf{d}) &= \|\mathbf{d}\|_1 = \sum |d_i| = \min && \text{optimization condition} \end{aligned} \right\},$$

↓
definition of the datum for the displacement vector

(18)

where $\mathbf{v}_{\Delta} \in \mathfrak{R}^{n \times 1}$ is the vector of residuals of differences in observations, $\mathbf{Q}_{\Delta} = (\mathbf{Q}_{(1)} + \mathbf{Q}_{(2)}) \in \mathfrak{R}^{n \times n}$ is the cofactor matrix of differences in observations and $\mathbf{P}_{\Delta} = \mathbf{Q}_{\Delta}^{-1} \in \mathfrak{R}^{n \times n}$ is the weight matrix of differences in observations.

To find the minimum of the first objective function $\phi(\mathbf{d})$, the classical technique based on the differential calculus can be applied. Determining the gradient of the objective function $\phi(\mathbf{d})$ and then using the necessary condition for the existence of a minimum of this function $(\partial\phi(\mathbf{d})/\partial\mathbf{d})^T = \mathbf{0}$, the following system of normal equations is obtained

$$\mathbf{N}_{\Delta}\mathbf{d} - \boldsymbol{\omega}_{\Delta} = \mathbf{0}, \quad (19)$$

where $\mathbf{N}_{\Delta} = \mathbf{A}^T \mathbf{P}_{\Delta} \mathbf{A}$, $\boldsymbol{\omega}_{\Delta} = \mathbf{A}^T \mathbf{P}_{\Delta} (\mathbf{I}_{(2)}^{\text{obs}} - \mathbf{I}_{(1)}^{\text{obs}})$. The objective function $\phi(\mathbf{d})$ is a convex function. Therefore, if the necessary condition is fulfilled, then the sufficient condition for a minimum of this function is fulfilled as well. The obtained system of normal Eq. (19) is, in fact, the set of permissible solutions (constraints) for vector \mathbf{d} , minimizing the objective function $\phi(\mathbf{d})$.

Continuing the solution of the optimization problem (18), we find the minimum of the second objective function $\psi(\mathbf{d})$, taking into account the constraints (19). The function $\psi(\mathbf{d})$ is not repeatedly differentiable and its minimum cannot be found using the classical technique, based on differential calculus, as minimization of this objective function requires the use of complex linear programming procedures (e.g., simplex method). For this reason, in this paper, the function $\psi(\mathbf{d})$ was replaced with an alternative, repeatedly differentiable function with the form (Kadaj 1988)

$$\psi_A(\mathbf{d}) = \sum_{i=1}^u \sqrt{d_i^2 + c^2}, \quad (20)$$

where c is the precision for computations, e.g., 0.0001 m. With the assumption that c is a numerically insignificant value, the component of the function $\psi_A(\mathbf{d})$ is equivalent to the component of the function $\psi(\mathbf{d})$ and then both functions are equivalent in terms of optimization properties. Objective function $\psi_A(\mathbf{d})$ is now repeatedly differentiable and its minimum can be found using the classical technique, based on differential calculus. According to the optimization theory, the method of Lagrangian multipliers can be applied to find the minimum of the objective function $\psi_A(\mathbf{d})$ with the constraints (19). According to this method, the objective function $\psi_A(\mathbf{d})$ with the constraints (19) is replaced by a secondary objective function without constraints (Lagrangian function)

$$L(\mathbf{d}) = \sum_{i=1}^u \sqrt{\hat{d}_i^2 + c^2} - \boldsymbol{\kappa}^T (\mathbf{N}_\Delta \mathbf{d} - \boldsymbol{\omega}_\Delta), \tag{21}$$

where $\boldsymbol{\kappa} \in \mathfrak{R}^{u \times 1}$ is the vector of Lagrangian multipliers. The necessary conditions for the existence of a minimum of the objective function $\psi_A(\mathbf{d})$ with the constraints (19) then have the following form (Kuhn–Tucker necessary conditions)

$$(\partial L(\mathbf{d}) / \partial \mathbf{d})^T = \mathbf{0} \tag{22}$$

$$\boldsymbol{\kappa}^T (\mathbf{N}_\Delta \mathbf{d} - \boldsymbol{\omega}_\Delta) = \mathbf{0} \tag{23}$$

The objective function $\psi_A(\mathbf{d})$ is a convex function. Therefore, if the above necessary conditions are fulfilled, the sufficient conditions for a minimum of this function are fulfilled as well. Determining the gradient of the function $L(\mathbf{d})$ and then using the necessary condition (22), the following equation is obtained

$$\mathbf{W} \hat{\mathbf{d}} - \mathbf{N}_\Delta \hat{\boldsymbol{\kappa}} = \mathbf{0} \tag{24}$$

where

$$\mathbf{W} = \text{diag} \left(\dots, 1/\sqrt{\hat{d}_i^2 + c^2}, \dots \right) \tag{25}$$

and $\mathbf{N}_\Delta^T = \mathbf{N}_\Delta$, $\mathbf{W}^T = \mathbf{W}$, because \mathbf{N}_Δ and \mathbf{W} are symmetrical matrices. The second necessary condition (23) can be replaced by the condition (19), (for $\hat{\boldsymbol{\kappa}} \neq \mathbf{0}$). Finally, after determination of vector $\hat{\mathbf{d}}$ from Eq. (24), the necessary condition (23) will assume the following form (system of normal equations of correlates)

$$\mathbf{M} \hat{\boldsymbol{\kappa}} - \boldsymbol{\omega}_\Delta = \mathbf{0}, \tag{26}$$

where $\mathbf{M} = \mathbf{N}_\Delta \mathbf{W}^{-1} \mathbf{N}_\Delta$. If vector $\hat{\boldsymbol{\kappa}}$ solves the system of Eq. (26), vector $\hat{\mathbf{d}}$ minimizes the objective function $\psi_A(\mathbf{d})$ with the constraints (19). Therefore, after determination of vector $\hat{\boldsymbol{\kappa}}$ from Eq. (26) and its substitution into Eq. (24), we finally obtain

$$\mathbf{W} \hat{\mathbf{d}} - \mathbf{N}_\Delta \mathbf{M}^{-1} \boldsymbol{\omega}_\Delta = \mathbf{0}, \tag{27}$$

where \mathbf{M}^{-1} is a g-inverse, such that $\mathbf{M} \mathbf{M}^{-1} \mathbf{M} = \mathbf{M}$. In the considered case of an FCN, \mathbf{A} is the matrix of the columnarly

incomplete rank (4), which is why the matrix \mathbf{M} is singular and there is no ordinary (classical) inverse \mathbf{M}^{-1} . To determine the g-inverse \mathbf{M}^{-} , according to g-inverse theory, the matrix $\mathbf{M} \in \mathfrak{R}^{u \times u}$ can be reduced to block form

$$\mathbf{M} = \begin{bmatrix} \mathbf{M}_{11} & \mathbf{M}_{12} \\ \mathbf{M}_{21} & \mathbf{M}_{22} \end{bmatrix} \rightarrow \mathbf{M}^{-} = \begin{bmatrix} \mathbf{M}_{11}^{-1} & \mathbf{0} \\ \mathbf{0} & \mathbf{0} \end{bmatrix}, \tag{28}$$

where $\mathbf{M}_{11} \in \mathfrak{R}^{r \times r}$ is a non-singular matrix with rank r . The g-inverse of the matrix \mathbf{M} is then the submatrix \mathbf{M}_{11}^{-1} , complemented with zeros to the dimension $\mathfrak{R}^{u \times u}$ (Rao 1973; Prószynski 1981). Of course, there are also other methods for determination of the g-inverse of this matrix. It can, therefore, be seen that we have here the problem of a datum defect for the geodetic network, which has not yet been solved. To reduce the matrix \mathbf{M} to the form (28), it is sufficient to represent the matrix \mathbf{A} in block form (5). Therefore, in this case, the problem of a datum defect for the geodetic network can be solved analogously as in the classical method, only in this case it is done simultaneously for both epochs. Moreover, let us recall that the same optimization conditions were also proposed in both methods. It can, therefore, be seen that both methods differ only in the functional models, i.e., (9) and (18), while the other theoretical assumptions are common. Returning to the computations, after substitution of the block matrix \mathbf{A} (5) into the matrix \mathbf{M} , we obtain

$$\mathbf{M}^{-} = \begin{bmatrix} (\mathbf{Q}_{11} \mathbf{W}_1^{-1} \mathbf{Q}_{11} + \mathbf{Q}_{12} \mathbf{W}_2^{-1} \mathbf{Q}_{12}^T)^{-1} & \mathbf{0} \\ \mathbf{0} & \mathbf{0} \end{bmatrix}, \tag{29}$$

where $\mathbf{Q}_{11} = \mathbf{A}_1^T \mathbf{P}_\Delta \mathbf{A}_1$, $\mathbf{Q}_{12} = \mathbf{A}_1^T \mathbf{P}_\Delta \mathbf{A}_2$ and $\mathbf{W} = \text{diag}(\mathbf{W}_1, \mathbf{W}_2)$. After substitution of the matrix (29) into the system of Eq. (27), we finally obtain

$$\mathbf{W} \hat{\mathbf{d}} - \mathbf{D}^T (\mathbf{D} \mathbf{W}^{-1} \mathbf{D}^T)^{-1} \mathbf{A}_1^T \mathbf{P}_\Delta (\mathbf{I}_{(2)}^{\text{obs}} - \mathbf{I}_{(1)}^{\text{obs}}) = \mathbf{0} \tag{30}$$

where $\mathbf{D} = [\mathbf{A}_1^T \mathbf{P}_\Delta \mathbf{A}_1 \quad \mathbf{A}_1^T \mathbf{P}_\Delta \mathbf{A}_2]$. We compute on the basis of the system of Eq. (30) the robust estimator of vector \mathbf{d} and its cofactor matrix. The computations are carried out in an iterative cycle with the following formula (approximate Newtonian process)

$$\left. \begin{aligned} \hat{\mathbf{d}}^{(k)} &= \mathbf{R}^{(k)} (\mathbf{I}_{(2)}^{\text{obs}} - \mathbf{I}_{(1)}^{\text{obs}}) \\ \mathbf{Q}_d^{(k)} &= \mathbf{R}^{(k)} (\mathbf{Q}_{(1)} + \mathbf{Q}_{(2)}) (\mathbf{R}^{(k)})^T \\ \mathbf{W}^{(k+1)} &= \text{diag} (\dots, w_i^{(k+1)}, \dots) \end{aligned} \right\}_{k=1,2,\dots} \tag{31}$$

where $\mathbf{R}^{(k)} = (\mathbf{W}^{(k)})^{-1} \mathbf{D}^T (\mathbf{D} (\mathbf{W}^{(k)})^{-1} \mathbf{D}^T)^{-1} \mathbf{A}_1^T \mathbf{P}_\Delta$ is the matrix of transformation of the vector of differences in observations into the displacement vector, $\mathbf{W}^{(k=1)} = \mathbf{I}$ and

$$w_i^{(k+1)} = 1/\sqrt{(\hat{d}_i^{(k)})^2 + c^2} \cong 1/(|\hat{d}_i^{(k)}| + c) \tag{32}$$

It should be stressed that there still remains problem of outlier detection (observations), which has not yet been solved. In

this case, this problem can be solved, e.g., on the basis of Baarda’s data snooping or Pope’s test, only in this case it is done on the basis of the vector of residuals of differences in observations from the first iterative step (31). Unfortunately, in this case, robust estimation “does not work” for detecting outliers (observations).

The iterative process (31) is finished when all components of the difference $|\hat{\mathbf{d}}^{(k+1)} - \hat{\mathbf{d}}^{(k)}|$ are lower than the adopted precision for computations c (convergence). The final robust estimator of the vector of displacement components for all analyzed points in an FCN, i.e., vector $\hat{\mathbf{d}}^R$ and the final cofactor matrix of this vector, i.e., matrix $\mathbf{Q}_{\hat{\mathbf{d}}^R}$, is obtained from the last iterative step.

3.2 Step 2: assessment of the significance of the displacement vector

Assessment of the significance of the vectors $\hat{\mathbf{d}}_i^R$ can of course be performed analogously as in the classical method, i.e., on the basis of the approximate global (13) and local (15) or (16) F tests. For the stochastic model of the REDOD method (18), the variance factor estimator has the following form

$$\hat{\sigma}_0^2 = \hat{\mathbf{v}}_{\Delta}^T \mathbf{P}_{\Delta} \hat{\mathbf{v}}_{\Delta} / (n - u + de) \tag{33}$$

4 Comparison of the classical IWST method with the proposed REDOD method

As previously mentioned, classical deformation analysis of FCN is most often performed by robust methods. The best known methods from this group include the IWST method. This method was used, among others, for deformation analysis of the Tevatron atomic particle accelerator complex at the Fermilab laboratory in the US and for deformation analysis of the world’s largest strip copper mine in Chile. The IWST method has also been implemented in the automated ALERT monitoring system developed by the Canadian Centre for Geodetic Engineering and in the universal GeoLab geodetic computation software. Section 2 describes the algorithm of classical robust methods. Particular attention was paid to the IWST method. In Sect. 3, a new robust deformation analysis method was proposed based on classical robust methods. This method was conventionally called REDOD.

The theoretical principles of the proposed REDOD method are very similar to the theoretical principles of the classical IWST method. Both methods have in common, among others, the definition of the datum for the geodetic network, i.e., the zero-variance computational base (5), the optimization condition for the displacement vector (the definition of the datum for the displacement vector), i.e., the minimal

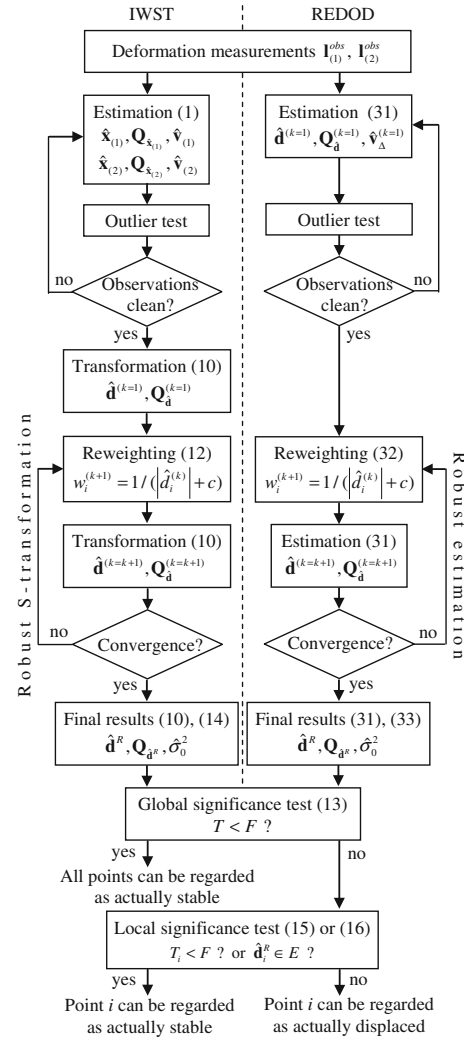


Fig. 1 Block diagram of the algorithms of the IWST and REDOD methods

L_1 -norm (9, 18), or the probabilistic model for the observations, i.e., normal distribution (2, 17).

The theoretical principles of both methods differ only in the functional deformation models, i.e., (9) and (18). Generally, the functional models (9) and (18) assume that the displacement vector is a function of differences in adjusted coordinates and differences in unadjusted observations, respectively. It is worth noting once more that the functional model (18) has some advantages which the functional model (9) does not have, namely, the functional model (18) accepts measurement errors constant in both epochs, which can be of any magnitude and may be different for individual geometric elements of the network. Moreover, unlike model (9), model (18) ensures stochastic consistency between the displacement vector estimator and the variance factor estimator. This results from the fact that both estimators are estimated here in the same computational process.

As a consequence of using different functional models, the algorithms of the IWST and REDOD methods differ significantly.

In Sects. 2 and 3, these algorithms were derived and described in detail. Only their basic aspects are shown below, in the form of a block diagram (Fig. 1).

5 Numerical tests

Numerical tests were performed on simulated FCN. The tests compared deformation analysis results obtained from the IWST and REDOD methods.

5.1 Example 1: deformation analysis of the leveling FCN

This test was performed on the example of a leveling network of four points A, B, C, D (Fig. 2). Computations were carried out for two variants of simulated observations.

First, the vector of theoretical heights of controlled points in epoch 1 $\mathbf{x}_{(1)} = [0.000, 0.000, 0.000, 0.000]^T$ m, the vector of theoretical displacements of controlled points $\mathbf{d} = [0, 10, 0, 0]^T$ mm and the vector of theoretical heights of controlled points in epoch 2 $\mathbf{x}_{(2)} = [0.000, 0.010, 0.000, 0.000]^T$ m were assumed. Theoretical height differences in both epochs were computed on the basis of the vectors $\mathbf{x}_{(1)}$ and $\mathbf{x}_{(2)}$.

In variant 1, the theoretical height differences were distorted with random errors according to the normal distribution and the significance level $\alpha = 0.05$. The same standard deviations of simulated errors of height difference measurement $\sigma_h = 4$ mm were assumed in both epochs.

In variant 2, the theoretical height differences were distorted with random errors from variant 1 and additionally with constant errors $\epsilon_h = +2$ mm.

The variants of simulated observations are presented in Table 1. Carrying out in succession the computations (10), (14), (13) and (15), complete results were obtained using IWST method. Carrying out in succession the computations (31), (33), (13) and (15) complete results were obtained using REDOD method. In both methods, constant heights z_D were assumed to eliminate the network's datum defect [Eq. (3) in the classical method and Eq. (27) in the proposed

Table 1 Simulated observations in epoch 1 and epoch 2

Observation designation		Variant (m)			
b	e	1		2	
		$\mathbf{l}_{(1)}^{obs}$	$\mathbf{l}_{(2)}^{obs}$	$\mathbf{l}_{(1)}^{obs}$	$\mathbf{l}_{(2)}^{obs}$
A	B	-0.003	0.014	-0.001	0.016
B	C	-0.004	-0.011	-0.002	-0.009
C	A	-0.001	0.006	0.001	0.008
A	D	0.002	-0.005	0.004	-0.003
D	C	-0.001	0.004	0.001	0.006
B	D	0.006	-0.009	0.008	-0.007

b beginning, *e* end

method], i.e., the submatrix \mathbf{A}_2 consisted of the $de = 1$ last column in the matrix \mathbf{A} , as was proposed in the theoretical part of this paper (5). Standard deviations of simulated errors of height difference measurement were assumed as a priori mean errors of height difference measurement. The values of a priori mean errors were the basis for determining the matrices $\mathbf{P}_{(1)}$, $\mathbf{P}_{(2)}$ (IWST) and \mathbf{P}_Δ (REDOD). Outlier detection was carried out using Baarda's method. The critical values were $\chi_{0.05}^2(3)/3 = 2.61$ and $t_{\alpha_0/2} = 2.51$ ($\beta_0 = 0.20$) for the global and local test, respectively. In variant 1, in the IWST method, the global test passed. In variant 2, in the IWST method, the global test failed in epoch 2 ($\hat{\sigma}_{0(2)}^2 = 2.89 > 2.61$), but the local test passed for all standardized residuals. In the REDOD method, the global test passed in both variants. In the IWST method, the test on the variance ratio passed in both variants [critical value $F(0.05, 3, 3) = 9.28$].

The results of the deformation analysis are presented in Table 2.

In variant 1, both methods give the same, correct results. In both methods, point B is considered unstable. In variant 2, in the IWST method, the value of vector $\hat{\mathbf{d}}^R$ is the same as in variant 1. Therefore, constant errors have no effect on vector $\hat{\mathbf{d}}^R$. However, the results of the assessment of significance are different than in variant 1. This is caused by the effect of constant errors. This effect was not eliminated from the values of the vectors $\hat{\mathbf{v}}_{(1)}$, $\hat{\mathbf{v}}_{(2)}$. This led to an increase in the value of $\hat{\sigma}_0^2$ (14), underestimation of the values of T (13), T_i (15) and, consequently, erroneous assessment of the significance of vector $\hat{\mathbf{d}}_B^R$. In the REDOD method, the effect of constant errors is eliminated. Both the value of vector $\hat{\mathbf{d}}^R$ and the results of the assessment of significance are the same as in variant 1.

5.2 Example 2: deformation analysis of the horizontal FCN

This test was performed on the example of a horizontal network of six points A, B, C, D, E, F (Fig. 3). Computations were carried out for four variants of simulated observations.

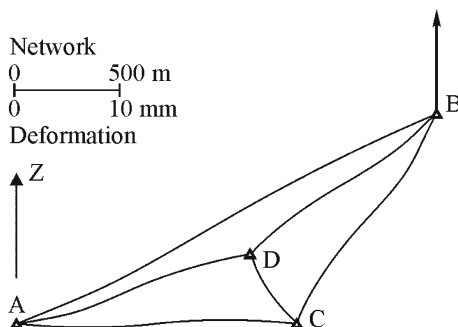
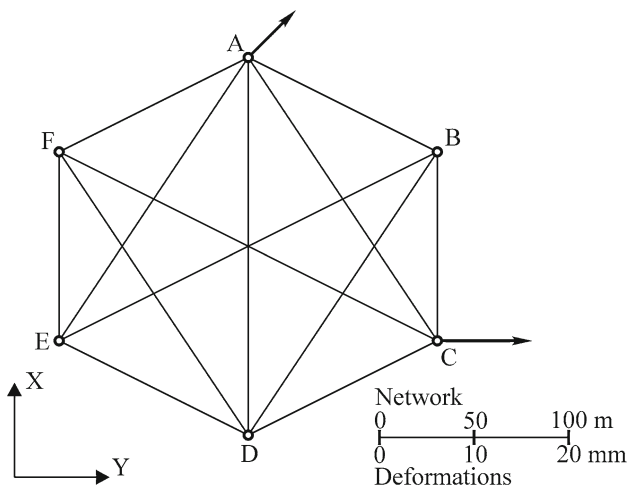


Fig. 2 Leveling FCN

Table 2 The results of the deformation analysis of the leveling FCN

Variant	Point	IWST					REDOD				
		$\hat{\mathbf{d}}_i^R = \hat{d}_{z_i^R}$ (mm)	$\hat{\sigma}_0^2$	$\sqrt{\mathbf{Q}\hat{\mathbf{d}}_i^R} = \sqrt{Q\hat{d}_{z_i^R}}$ (m)	T	T_i	$\hat{\mathbf{d}}_i^R = \hat{d}_{z_i^R}$ (mm)	$\hat{\sigma}_0^2$	$\sqrt{\mathbf{Q}\hat{\mathbf{d}}_i^R} = \sqrt{Q\hat{d}_{z_i^R}}$ (m)	T	T_i
1	A	0.5	1.01	0.0014	6.03 ^a	0.12	0.5	1.05	0.0014	5.79 ^a	0.11
	B	11.0		0.0033		10.61 ^a	11.0		0.0033		10.19 ^a
	C	-1.0		0.0026		0.15	-1.0		0.0026		0.14
	D	-5.5		0.0033		2.79	-5.5		0.0033		2.68
2	A	0.5	1.88	0.0014	3.23	0.06	0.5	1.05	0.0014	5.79 ^a	0.11
	B	11.0		0.0033		5.68	11.0		0.0033		10.19 ^a
	C	-1.0		0.0026		0.08	-1.0		0.0026		0.14
	D	-5.5		0.0033		1.50	-5.5		0.0033		2.68

^a The test statistic exceeds the critical value for the local $F(0.05, 1, 6) = 5.99$ or global $F(0.05, 3, 6) = 4.76$ test

**Fig. 3** Horizontal FCN

First, the vector of theoretical coordinates of controlled points in epoch 1 $\mathbf{x}_{(1)} = [350.000, 200.000, 300.000, 300.000, 200.000, 300.000, 150.000, 200.000, 200.000, 100.000, 300.000, 100.000]^T$ m, the vector of theoretical displacements of controlled points $\mathbf{d} = [5, 5, 0, 0, 0, 10, 0, 0, 0, 0, 0, 0]^T$ mm and the vector of theoretical coordinates of controlled points in epoch 2 $\mathbf{x}_{(2)} = [350.005, 200.005, 300.000, 300.000, 200.000, 300.010, 150.000, 200.000, 200.000, 100.000, 300.000, 100.000]^T$ m were assumed.

In variant 1, observations were distorted with random errors. Theoretical observations were computed on the basis of the vectors $\mathbf{x}_{(1)}$, $\mathbf{x}_{(2)}$. The theoretical observations were then distorted with random errors according to the normal distribution and the significance level $\alpha = 0.05$. The same standard deviations of simulated errors of angle measurement $\sigma_\beta = 10^{\text{cc}}$ and distance measurement $\sigma_s = 3$ mm were assumed in both epochs.

In variant 2, observations were also distorted with random errors. Theoretical observations were computed on the basis

of the vectors $\mathbf{x}_{(1)}$, $\mathbf{x}_{(2)}$. The theoretical observations were then distorted with random errors according to the normal distribution and the significance level $\alpha = 0.05$. However, different standard deviations of simulated errors of angle measurement were assumed in both epochs in this case. In epoch 1, the standard deviation of angle measurement errors at central points A, B, C $\sigma_\beta = 15^{\text{cc}}$, at central points D, E, F $\sigma_\beta = 5^{\text{cc}}$ and the standard deviation of distance measurement errors $\sigma_s = 3$ mm were assumed. In epoch 2, the standard deviation of angle measurement errors at central points A, B, C $\sigma_\beta = 5^{\text{cc}}$, at central points D, E, F $\sigma_\beta = 15^{\text{cc}}$ and the standard deviation of distance measurement errors $\sigma_s = 3$ mm were assumed.

In variant 3, observations were distorted with random errors and constant errors. The vector $\varepsilon_x = [3, 3, 3, 3, 3, 3, 3, 3, 3, 3, 3, 3]^T$ mm was added to the vectors $\mathbf{x}_{(1)}$, $\mathbf{x}_{(2)}$ and the vectors of eccentric coordinates of the target $\mathbf{x}_{(1)}^e$, $\mathbf{x}_{(2)}^e$ were obtained. The eccentric observations were then computed on the basis of the theoretical coordinates of the instrument $\mathbf{x}_{(1)}$, $\mathbf{x}_{(2)}$ and the eccentric coordinates of the target $\mathbf{x}_{(1)}^e$, $\mathbf{x}_{(2)}^e$. In other words, observations distorted by constant errors in the form of eccentricity of the target in relation to the instrument with the value of $\varepsilon_x = +3$ mm along the axes X and Y were obtained this way. These observations were then additionally distorted with random errors from variant 1.

In variant 4, observations were distorted with constant errors from variant 3 and random errors from variant 2.

The variants of simulated observations are presented in Table 3.

Complete results were obtained in the IWST method by carrying out the computations (10), (14), (13) and (16) in succession. Complete results were obtained in the REDOD method by carrying out the computations (31), (33), (13) and (16) in succession. In both methods, constant coordinates y_E , x_F , y_F were assumed to eliminate the network's datum defect (Eq. (3) in the classical method and Eq. (27)

Table 3 Simulated observations in epoch 1 and epoch 2

Observation designation			Variant (g), (m)							
c	l	r	1		2		3		4	
			I ^{obs} ₍₁₎	I ^{obs} ₍₂₎	I ^{obs} ₍₁₎	I ^{obs} ₍₂₎	I ^{obs} ₍₁₎	I ^{obs} ₍₂₎	I ^{obs} ₍₁₎	I ^{obs} ₍₂₎
A	B	C	33.0507	33.0457	33.0510	33.0455	33.0515	33.0465	33.0518	33.0463
A	C	D	37.4338	37.4364	37.4344	37.4360	37.4343	37.4369	37.4349	37.4364
A	D	E	37.4354	37.4320	37.4354	37.4329	37.4361	37.4327	37.4361	37.4336
A	E	F	33.0503	33.0473	33.0500	33.0477	33.0513	33.0484	33.0510	33.0488
B	C	D	37.4328	37.4402	37.4332	37.4404	37.4344	37.4418	37.4348	37.4420
B	D	E	33.0501	33.0488	33.0507	33.0495	33.0507	33.0494	33.0513	33.0501
B	E	A	59.0319	59.0370	59.0332	59.0368	59.0339	59.0389	59.0352	59.0387
C	D	F	59.0341	59.0289	59.0340	59.0292	59.0345	59.0293	59.0344	59.0296
C	F	A	33.0512	33.0513	33.0488	33.0496	33.0515	33.0516	33.0491	33.0499
C	A	B	37.4351	37.4277	37.4333	37.4282	37.4355	37.4282	37.4337	37.4287
D	E	F	33.0504	33.0522	33.0498	33.0492	33.0495	33.0513	33.0489	33.0483
D	F	A	37.4327	37.4338	37.4338	37.4356	37.4322	37.4333	37.4333	37.4351
D	A	B	37.4359	37.4326	37.4335	37.4303	37.4352	37.4320	37.4328	37.4297
D	B	C	33.0510	33.0527	33.0508	33.0509	33.0499	33.0517	33.0497	33.0499
E	F	A	37.4333	37.4326	37.4331	37.4332	37.4317	37.4310	37.4315	37.4316
E	A	B	33.0491	33.0508	33.0497	33.0512	33.0484	33.0501	33.0490	33.0505
E	B	D	59.0337	59.0331	59.0338	59.0325	59.0318	59.0312	59.0319	59.0306
F	A	C	59.0316	59.0332	59.0335	59.0310	59.0313	59.0329	59.0333	59.0307
F	C	D	33.0509	33.0512	33.0500	33.0528	33.0505	33.0509	33.0496	33.0525
F	D	E	37.4343	37.4342	37.4336	37.4339	37.4339	37.4338	37.4332	37.4335
-	A	B	111.804	111.807	111.801	111.801	111.806	111.809	111.803	111.803
-	B	C	100.007	99.993	99.993	99.997	100.004	99.990	99.990	99.994
-	C	D	111.801	111.811	111.800	111.807	111.797	111.807	111.796	111.803
-	D	E	111.798	111.802	111.802	111.804	111.797	111.801	111.801	111.803
-	E	F	100.001	100.001	99.999	99.997	100.004	100.004	100.002	100.000
-	F	A	111.804	111.812	111.805	111.809	111.808	111.816	111.809	111.813

c central, l left, r right

in the proposed method), i.e., the submatrix **A**₂ consisted of the *de* = 3 last columns in the matrix **A**, as was proposed in the theoretical part of this paper (5). The theoretical coordinates from epoch 1 were assumed as approximate coordinates. Standard deviations of simulated errors of angle and distance measurement were assumed as a priori mean errors of angle and distance measurement. The values of a priori mean errors were the basis for determining the matrices **P**₍₁₎, **P**₍₂₎ (IWST) and **P**_Δ (REDOD). Outlier detection was carried out by Baarda's method. The critical values were $\chi^2_{0.05}(17)/17 = 1.62$ and $t_{\alpha_0/2} = 3.63$ ($\beta_0 = 0.20$) for the global and local test, respectively. The global test passed in variants 1 and 2 in the IWST method, but the global test failed in both epochs in variant 3 in the IWST method ($\hat{\sigma}^2_{0(1)} = 2.51 > 1.62$, $\hat{\sigma}^2_{0(2)} = 2.10 > 1.62$), although the local test passed for all standardized residuals. In variant 4, in the IWST method, the global test failed in both epochs

($\hat{\sigma}^2_{0(1)} = 2.98 > 1.62$, $\hat{\sigma}^2_{0(2)} = 3.42 > 1.62$) and the local test failed in both epochs. The largest standardized residuals of epochs 1 and 2 were $\hat{v}_{DEF}/\sigma_{\hat{v}_{DEF}} = 4.51 > 3.63$ and $\hat{v}_{ABC}/\sigma_{\hat{v}_{ABC}} = 5.36 > 3.63$, respectively. These observations were deleted. The critical values at that point were $\chi^2_{0.05}(16)/16 = 1.64$ and $t_{\alpha_0/2} = 3.58$ ($\beta_0 = 0.20$) for the global and local test, respectively. In the IWST method, the global test failed again in both epochs ($\hat{\sigma}^2_{0(1)} = 1.98 > 1.64$, $\hat{\sigma}^2_{0(2)} = 1.92 > 1.64$), but the local test passed now for all standardized residuals. In the REDOD method, the global test passed in all variants. In the IWST method, the test on the variance ratio passed in all variants [critical value $F(0.05, 17, 17) = 2.27$].

The results of deformation analysis are presented in Table 4.

In variant 1, both methods yield the same results (within the limits of accuracy of computations).

Table 4 The results of deformation analysis of the horizontal FCN

Variant	Point	IWST						REDOD					
		$\hat{\sigma}_0^2$		$\sqrt{Q\hat{a}_i^R} =$		$E =$		$\hat{\sigma}_0^2$		$\sqrt{Q\hat{a}_i^R} =$		$E =$	
		$\begin{bmatrix} \hat{d}x_i^R \\ \hat{d}y_i^R \end{bmatrix}$ (mm)		$\begin{bmatrix} \sqrt{Q\hat{d}x_i^R} \\ \sqrt{Q\hat{d}y_i^R} \end{bmatrix}$ (m)		a_i b_i (mm)	φ_i (g)			$\begin{bmatrix} \sqrt{Q\hat{d}x_i^R} \\ \sqrt{Q\hat{d}y_i^R} \end{bmatrix}$ (m)		a_i b_i (mm)	φ_i (g)
1	A	7.1	1.13	0.0025	0.0010	6.9	16	7.1	1.10	0.0025	0.0011	6.9	18
		4.1		0.0010	0.0016	4.1		4.0		0.0011	0.0016	4.1	
	B	-2.4		0.0021	0.0017	7.8	-44	-2.4		0.0021	0.0017	7.8	-41
		-0.6		0.0017	0.0024	4.0		-0.7		0.0017	0.0025	4.1	
	C	1.0		0.0011	0.0001	7.3	0	1.0		0.0011	-0.0004	7.3	2
		10.2		0.0001	0.0027	3.1		10.1		-0.0004	0.0027	3.0	
	D	0.4		0.0013	-0.0011	5.3	36	0.4		0.0014	-0.0011	5.2	36
		-1.3		-0.0011	0.0017	2.8		-1.4		-0.0011	0.0017	2.8	
	E	-0.8		0.0012	0.0007	3.9	48	-0.8		0.0013	0.0007	3.9	46
		-0.7		0.0007	0.0012	2.7		-0.7		0.0007	0.0012	2.7	
	F	-0.8		0.0016	-0.0011	4.9	-35	-0.7		0.0016	-0.0011	4.9	-35
		0.2		-0.0011	0.0012	2.1		0.2		-0.0011	0.0011	2.0	
2	A	4.8	0.73	0.0026	-0.0015	6.1	-28	5.1	0.74	0.0028	-0.0008	6.2	-10
		2.9		-0.0015	0.0017	2.9		3.7		-0.0008	0.0019	4.1	
	B	-0.3		0.0022	0.0013	5.2	23	-0.2		0.0018	0.0013	4.8	41
		0.1		0.0013	0.0010	1.4		0.2		0.0013	0.0015	2.1	
	C	1.6		0.0013	0.0008	3.9	-30	2.1		0.0018	0.0006	4.3	-36
		10.1		0.0008	0.0016	2.5		10.4		0.0006	0.0019	3.8	
	D	0.0		0.0010	-0.0003	2.3	-23	0.0		0.0012	-0.0004	3.6	7
		-0.1		-0.0003	0.0009	1.9		-0.4		-0.0004	0.0016	2.6	
	E	-0.1		0.0011	0.0011	5.1	-17	0.0		0.0008	0.0003	5.1	-1
		-1.7		0.0011	0.0022	2.0		-1.1		0.0003	0.0023	1.8	
	F	-0.2		0.0015	-0.0016	6.2	28	-0.9		0.0024	-0.0016	6.4	48
		-1.7		-0.0016	0.0026	2.4		-1.4		-0.0016	0.0024	4.0	
3	A	7.1	2.30	0.0025	0.0010	9.9	16	7.1	1.10	0.0025	0.0011	6.9	18
		4.1		0.0010	0.0016	5.9		4.0		0.0011	0.0016	4.1	
	B	-2.4		0.0021	0.0017	11.2	-44	-2.4		0.0021	0.0017	7.8	-41
		-0.6		0.0017	0.0024	5.8		-0.7		0.0017	0.0025	4.1	
	C	1.0		0.0011	0.0001	10.5	0	1.0		0.0011	-0.0004	7.3	2
		10.2		0.0001	0.0027	4.5		10.1		-0.0004	0.0027	3.0	
	D	0.4		0.0013	-0.0011	7.6	36	0.4		0.0014	-0.0011	5.2	36
		-1.3		-0.0011	0.0017	4.0		-1.4		-0.0011	0.0017	2.8	
	E	-0.8		0.0012	0.0007	5.6	48	-0.8		0.0013	0.0007	3.9	46
		-0.7		0.0007	0.0012	3.9		-0.7		0.0007	0.0012	2.7	
	F	-0.8		0.0016	-0.0011	7.1	-35	-0.7		0.0016	-0.0011	4.9	-35
		0.2		-0.0011	0.0012	3.0		0.2		-0.0011	0.0011	2.0	
4	A	3.5	1.95	0.0022	-0.0017	10.0	-46	5.1	0.74	0.0028	-0.0008	6.2	-10
		1.4		-0.0017	0.0021	4.5		3.7		-0.0008	0.0019	4.1	
	B	-6.2		0.0028	0.0010	10.0	9	-0.2		0.0018	0.0013	4.8	41
		0.0		0.0010	0.0005	1.1		0.2		0.0013	0.0015	2.1	

Table 4 continued

Variant	Point	IWST				REDOD					
		$\hat{\mathbf{d}}_i^R = \begin{bmatrix} \hat{d}_{x_i^R} \\ \hat{d}_{y_i^R} \end{bmatrix}$ (mm)	$\hat{\sigma}_0^2$	$\sqrt{\mathbf{Q}_{\hat{\mathbf{d}}_i^R}} = \begin{bmatrix} \sqrt{Q_{\hat{d}_{x_i^R}}} & \sqrt{Q_{\hat{d}_{x_i^R}\hat{d}_{y_i^R}}} \\ \sqrt{Q_{\hat{d}_{y_i^R}\hat{d}_{x_i^R}}} & \sqrt{Q_{\hat{d}_{y_i^R}}} \end{bmatrix}$ (m)	$E = \begin{matrix} a_i & b_i & \varphi_i \\ \text{(mm)} & & \text{(g)} \end{matrix}$	$\hat{\mathbf{d}}_i^R = \begin{bmatrix} \hat{d}_{x_i^R} \\ \hat{d}_{y_i^R} \end{bmatrix}$ (mm)	$\hat{\sigma}_0^2$	$\sqrt{\mathbf{Q}_{\hat{\mathbf{d}}_i^R}} = \begin{bmatrix} \sqrt{Q_{\hat{d}_{x_i^R}}} & \sqrt{Q_{\hat{d}_{x_i^R}\hat{d}_{y_i^R}}} \\ \sqrt{Q_{\hat{d}_{y_i^R}\hat{d}_{x_i^R}}} & \sqrt{Q_{\hat{d}_{y_i^R}}} \end{bmatrix}$ (m)	$E = \begin{matrix} a_i & b_i & \varphi_i \\ \text{(mm)} & & \text{(g)} \end{matrix}$	a_i	b_i
C	1.3	0.0013	0.0009	6.4	-31	2.1	0.0018	0.0006	4.3	-36	
	11.8	0.0009	0.0016	4.0		10.4	0.0006	0.0019	3.8		
D	-1.0	0.0014	0.0000	4.9	0	0.0	0.0012	-0.0004	3.6	7	
	0.1	0.0000	0.0002	0.9		-0.4	-0.0004	0.0016	2.6		
E	2.3	0.0021	0.0014	9.4	-43	0.0	0.0008	0.0003	5.1	-1	
	-2.8	0.0014	0.0023	6.2		-1.1	0.0003	0.0023	1.8		
F	-1.8	0.0015	-0.0010	10.7	10	-0.9	0.0024	-0.0016	6.4	48	
	-4.5	-0.0010	0.0029	5.2		-1.4	-0.0016	0.0024	4.0		

In both methods, the global significance test of the displacement vector T (13) failed for all variants

In variant 2, the values of vector $\hat{\mathbf{d}}^R$ and the parameters of confidence ellipses differ in both methods. This is caused by disproportionateness of the matrices $\mathbf{P}_{(1)}$, $\mathbf{P}_{(2)}$ (IWST) to the matrix \mathbf{P}_Δ (REDOD). However, these differences are not significant. Moreover, the sum of absolute values of true errors for the components of vector $\hat{\mathbf{d}}^R$ is the same in both methods, $\sum |\hat{d}_i^R - d_i| = 8.2$ mm.

In variant 3, in the IWST method, the value of vector $\hat{\mathbf{d}}^R$ is the same as in variant 1. Therefore, constant errors have no effect on vector $\hat{\mathbf{d}}^R$. However, the values of the parameters of confidence ellipses differ significantly from the values in variant 1. This is caused by the effect of constant errors. This effect was not eliminated from the values of the vectors $\hat{\mathbf{v}}_{(1)}$, $\hat{\mathbf{v}}_{(2)}$. This led to an increase in the value of $\hat{\sigma}_0^2$ (14) and, consequently, to an increase in the values of the parameters of confidence ellipses (16). In the REDOD method, the effect of constant errors is eliminated. Both the values of vector $\hat{\mathbf{d}}^R$ and the values of the parameters of confidence ellipses are the same as in variant 1.

In variant 4, in the IWST method, the value of vector $\hat{\mathbf{d}}^R$ differs significantly from the value in variant 2. The sum of absolute values of true errors for the values of vector $\hat{\mathbf{d}}^R$ is significantly higher than in variant 2, $\sum |\hat{d}_i^R - d_i| = 26.9$ mm. This is caused by the disproportion of matrix $\mathbf{P}_{(1)}$ to matrix $\mathbf{P}_{(2)}$. This in turn led to a disproportionate effect of constant errors on the values of the vectors $\hat{\mathbf{x}}_{(1)}$, $\hat{\mathbf{x}}_{(2)}$ (1) and, consequently, prevented complete reduction of these errors in the iterative process (10). The values of the parameters of confidence ellipses also differ significantly from the values in variant 2. As in variant 3, this is caused by the effect of

constant errors on the value of $\hat{\sigma}_0^2$. In the REDOD method, the effect of constant errors is eliminated. Both the values of vector $\hat{\mathbf{d}}^R$ and the values of the parameters of confidence ellipses are the same as in variant 2.

Figure 4 presents graphical assessment of the significance of vector $\hat{\mathbf{d}}^R$ (16).

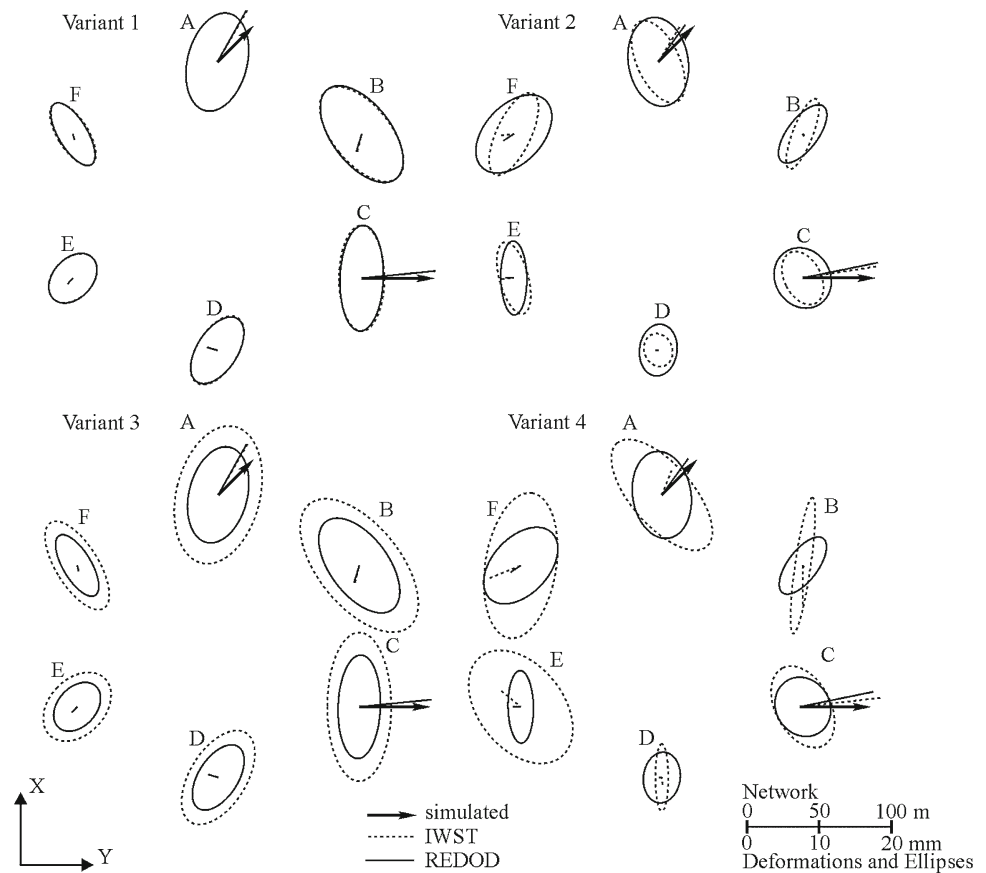
In the case of the occurrence of only random errors (Fig. 4, variants 1, 2), the results of assessment of significance are correct in both methods. The displacements of points A and C are considered significant in both variants.

In the case of the occurrence of random errors and constant errors (Fig. 4, variants 3, 4), the results of assessment of significance in the IWST method are not correct. Only the displacement of point C is considered significant in both variants. This is caused by the effect of constant errors. In the REDOD method, the results of assessment of significance are correct. The displacements of points A and C are considered significant in both variants.

6 Summary and conclusions

Deformation measurements have a repeatable nature. In other words, deformation measurements are performed at different moments of time, but often with the same equipment, methods, geometric conditions and in a similar environment in epochs 1 and 2. Moreover, the same instrument and target are most often set on given points in both epochs. It is, therefore, reasonable to assume that the results of deformation measurements can be distorted both by random errors and by some non-random errors, which are constant in both

Fig. 4 The results of assessment of the significance of displacements in the case of the occurrence of random errors (variants 1, 2) and in the case of the occurrence of random and constant errors (variants 3, 4)



epochs, i.e., errors with the same value and the same sign in both epochs. There may be constant errors which cannot be eliminated from measurement results, e.g., incompletely reduced atmospheric refraction, eccentricity of the target in relation to the instrument (caused by faulty execution or assembly, non-vertical mounting of the centering sleeve in the instrument pillar or inclination of the instrument pillar with time). There may also be constant errors which can be eliminated from measurement results although, for example, economic and technical limitations of the measurement project prevent their elimination (Caspary 2000). For example, a pillar could have a GNSS mounted, as well as a target prism that RTS could observe (Fig. 5). In this case, the target prism and GNSS receiver cannot define the same physical point.

For FCN, the results of deformation measurements are most often processed using the robust methods. Classical robust methods do not completely eliminate the effect of constant errors and, therefore, lead to reduced external reliability level of processing and, consequently, to reduced quality of deformation analysis results.

This paper proposes a new robust alternative method, which was called REDOD. The performed numerical tests showed that:

1. If the results of deformation measurements were additionally distorted by constant errors, the REDOD method completely eliminated their effect from deformation analysis results,
2. If the results of deformation measurements were distorted only by random errors, the REDOD method yielded very similar deformation analysis results as the classical IWST method.

The REDOD method was developed for FCN, which has the same observation structure in both epochs. That is, the same geometric elements must be measured in the control network in both epochs. For example, this condition is always met for automated, continuous control measurements. As previously mentioned, there is a high risk that the error of measurement of the same geometric element of the network in both epochs may contain a factor constant in both epochs and, therefore, the REDOD method is strongly recommended in this case.

It should be noted, however, that sometimes, in practice, control networks have a different observation structure in both epochs. For example, the classical technique in epoch 1 can be replaced with the GNSS technique in epoch 2. In this case, the REDOD method can also be used. The input data for

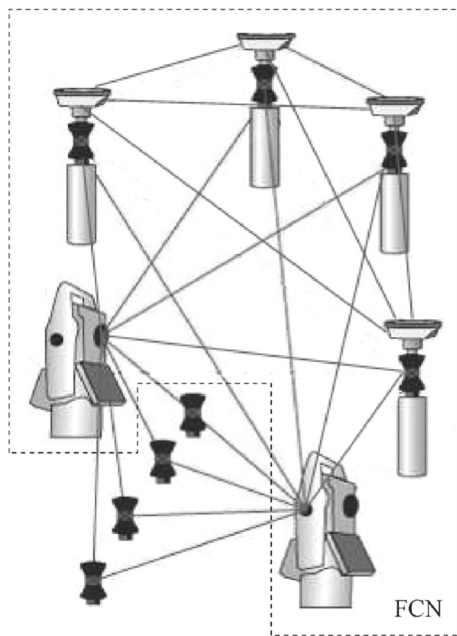


Fig. 5 Integrated deformation measurements (RTS, target prism and GNSS receiver) for network of potential reference points (FCN)

the REDOD method will then be pseudo-observations of the same geometric elements of the network in both epochs (e.g., vectors). Such pseudo-observations can be computed based on preadjusted coordinates. However, it should be noted that for networks which have different observation structure in both epochs, there is a very low risk that error constant in both epochs will occur and, therefore, in this case, the REDOD method is not strongly recommended. As previously demonstrated, if there are no error constant in both epochs, the REDOD and IWST methods give much the same quality of deformation analysis results.

he obtained results encourage further research into the latest robust solutions for deformation estimation from observation differences. The method of sign-constrained robust least squares, which detects over 50 % of outliers (Xu 2005), and robust estimation by expectation maximization algorithm, which is more sensitive to outliers than classical methods (Koch 2013; Koch and Kargoll 2013), may be particularly useful. Moreover, new numerical tests should be performed for new approaches, based on many thousands of simulated data sets (e.g., Monte Carlo simulations). Not only measurement errors should be randomized in individual sets, but also the number and location of displaced points and the values and directions of these points' displacements. The measure of accuracy of the estimated displacements could be empirical standard deviation and the measure of significance test efficiency could be the mean success rate (MSR) (Hekimoglu and Koch 1999).

Acknowledgments The authors wish to thank the editors and three anonymous reviewers for their time, effort and help in improving the manuscript.

Open Access This article is distributed under the terms of the Creative Commons Attribution License which permits any use, distribution, and reproduction in any medium, provided the original author(s) and the source are credited.

References

- Aydin C (2013) Power of global test in deformation analysis. *J Surv Eng* 138(2):51–55
- Casparly WF (1984) Deformation analysis using a special similarity transformation. In: *FIG Int Eng Surv Conf*, Washington DC, pp 145–151
- Casparly WF, Borutta H (1987) Robust estimation in deformation models. *Surv Rev* 29(223):29–45
- Casparly WF, Haen W, Borutta H (1990) Deformation analysis by statistical methods. *Technometrics* 39(1):49–57
- Casparly WF (2000) Concepts of network and deformation analysis. The University of New South Wales, Kensington
- Cederholm P (2003) Deformation analysis using confidence ellipsoids. *Surv Rev* 37(287):31–45
- Chen YQ (1983) Analysis of deformation surveys- a generalized method. Technical Report No. 94 University of New Brunswick, Fredericton, pp 54–72
- Chen YG, Chrzanowski A, Secord JM (1990) A strategy for the analysis of the stability of reference points in deformation surveys. *CISM J ACSGG* 44(2):141–149
- Chrzanowski A, Chen YQ (1990) Deformation monitoring, analysis and prediction-status report FIG XIX international congress. *Helsinki* 6(604.1):83–97
- Denli HH, Deniz R (2003) Global congruency test methods for GPS networks. *J Surv Eng* 129(3):95–98
- Denli HH (2008) Stable point research on deformation networks. *Surv Rev* 40(307):74–82
- Du Mond CE, Lenth RV (1987) A robust confidence interval for location. *Technometrics* 29(2):211–219
- Duchnowski R (2010) Median-based estimates and their application in controlling reference mark stability. *J Surv Eng* 136(2):47–52
- Duchnowski R, Wiśniewski Z (2012) Estimation of the shift between parameters of functional models of geodetic observations by applying M_{split} estimation. *J Surv Eng* 138(1):1–8
- Duchnowski R (2013) Hodges–Lehmann estimates in deformation analyses. *J Geod* 87(10–12):873–884
- Even-Tzur G (2011) Deformation analysis by means of extended free network adjustment constraints. *J Surv Eng* 137(2):47–52
- Gökalp E, Taşçi L (2009) Deformation monitoring by GPS at embankment dams and deformation analysis. *Surv Rev* 41(311):86–102
- Hekimoglu S, Koch KR (1999) How can reliability of robust methods be measured? Third Turkish-German Joint Geodetic Days, Istanbul 1:179–196
- Kadaj R (1988) Eine Klasse von Schätzverfahren mit praktischen Anwendungen. *Zeitschrift für Vermessungswesen* H8(117J):157–165
- Kamiński W, Nowel K (2013) Local variance factors in deformation analysis of non-homogenous monitoring networks. *Surv Rev* 45(328):44–50
- Koch KR (2013) Robust estimation by expectation maximization algorithm. *J Geod* 87(2):107–116
- Koch KR, Kargoll B (2013) Expectation maximization algorithm for the variance-inflation model by applying the t-distribution. *J Appl Geod* 7:217–225

- Lazzarini T, Laudyn I, Chrzanowski A, Gaździcki J, Janusz W, Wilun Z, Mayzel B, Mikucki Z (1977) Geodetic measurements of displacements of structures and their surroundings. PPWK, Warsaw (in Polish)
- Marx C (2013) On resistant L_p -norm estimation by means of iteratively reweighted least squares. *J Appl Geod* 7:1–10
- Niemeier W (1981) Statistical tests for detecting movements in repeatedly measured geodetic networks. *Tectonophysics* 71(1981):335–351
- Prószyński W (1981) Introduction into applications of the generalized Moore–Penrose inverse to chosen adjustment problems. *Geod Cartogr* 4(2):123–130
- Prószyński W (2010) Another approach to reliability measures for systems with correlated observations. *J Geod* 84(9):547–556
- Rao RC (1973) *Linear statistical inference and its applications*. Wiley, New York
- Setan H, Othman R (2006) Monitoring of offshore platform subsidence using permanent GPS stations. *J Glob Position Syst* 5(1–2):17–21
- Setan H, Singh R (2001) Deformation analysis of a geodetic monitoring network. *Geomatica* 55(3):333–346
- Wilkins R, Bastin G, Chrzanowski A (2003) ALERT: a fully automated real time monitoring system. In: FIG XI symposium on deformation measurements, Greece
- Wiśniewski Z (2009) Estimation of parameters in a split functional model of geodetic observations (M_{split} estimation). *J Geod* 83(2):105–120
- Xu PL (2005) Sign-constrained robust least squares, subjective breakdown point and the effect of weights of observations on robustness. *J Geod* 79(1–3):146–159